# Extragalactic Gamma-Ray Absorption and the Intrinsic Spectrum of Mkn 501 during the 1997 Flare.

O.C. de Jager

Unit for Space Physics, Potchefstroom University for CHE, Potchefstroom 2520, South Africa

F.W. Stecker

Laboratory for High Energy Astrophysics, NASA Goddard Space Flight Center, Greenbelt, MD 20771, USA

# ABSTRACT

Using the recent models of Malkan & Stecker (2001) for the infrared background radiation and extrapolating them into the optical and UV range using recent galaxy count data, we rederive the optical depth of the Universe to high energy  $\gamma$ -rays as a function of energy and redshift for energies betweeen 50 GeV and 100 TeV and redshifts between 0.03 and 0.3. We then use these results to derive the intrinsic  $\gamma$ -ray spectrum of Mkn 501 during its 1997 high state. We find that the time averaged spectral energy distribution of Mkn 501 while flaring had a broad, flat peak in the  $\sim 5-10$  TeV range which corresponds to the broad, flat time averaged X-ray peak in the  $\sim 50-100$  keV range observed during the flare. The spectral index of our derived intrinsic differential photon spectrum for Mkn 501 at energies below  $\sim 2$  TeV was found to be  $\sim 1.6-1.7$ . This corresponds to a time averaged spectral index of 1.76 found in soft X-rays at energies below the X-ray (synchrotron) peak. These results appear to favor a synchrotron-self Compton (SSC) origin for the TeV emission together with jet parameters which are consistent with time variability constraints within the context of a simple SSC model.

*Subject headings:* gamma-rays: theory - BL Lacertae objects: individual: Mkn 501 - cosmology: diffuse radiation - galaxies: intergalactic medium

# 1. Introduction

The spectra of high energy  $\gamma$ -rays from extragalactic sources are predicted to be modified by strongly redshift dependent absorption effects caused by interactions of these  $\gamma$ -rays with photons of the intergalactic IR-UV background radiation (Stecker, De Jager & Salamon 1992). Several attempts have been made to infer the IR SED (spectral energy distribution) either from model calculations or observations. (See Hauser & Dwek (2001) for the latest review.) Such information can be used to calculate the optical depth for TeV range photons as a function of energy and redshift so that the intrinsic spectrum of an observed source can be derived.

Of particular interest is the spectrum of Mkn 501 which was observed while strongly flaring in 1997. The spectrum observed at that time by the *HEGRA* air Cherenkov telescope system (Aharonian, *et al.* 1999, 2001a) extended to energies greater than 20 TeV, the highest energies yet observed from an extragalactic source.

Application of the Stecker & de Jager (1998) calculations for the optical depth to the observed spectrum as first reported reported by Aharonian, *et al.* (1999) resulted in an intrinsic spectrum which was consistent with a differential power-law form for the photon spectrum  $\propto E^{-2}$  between 0.5 and 20 TeV, corresponding to a flat spectral energy distribution (SED), *i.e.*,  $E^2[dN/dE] \simeq \text{constant}$  (Konopelko, Kirk, Stecker & Mastichiadas 1999). In this paper, we will rederive the intrinsic spectrum of Mkn 501 using the method employed by Konopelko, *et al.* (1999) by using the recalibrated observed spectrum as given by Aharonian *et al.* (2001a) and using a consistent hybrid model for the extragalactic background radiation. We correct for absorption by first recalculating the opacity of intergalactic space to  $\gamma$ -rays,  $\tau(E, z)$ , using the new calculations of the IR background spectrum of Malkan & Stecker (2001) extended into the optical domain as described later in this paper. The consistency between the *Whipple* telescope and *HEGRA* spectra of Mkn 501 allows us to derive the intrinsic spectrum of Mkn 501 over two decades of energy.

The intrinsic TeV  $\gamma$ -ray SED which we derive here,  $\nu F(\nu) = E^2[dN/dE]$ , is again quite flat. However, it is slightly convex, with a broad peak in the multi-TeV range. The spectrum can be interpreted as a Compton peak corresponding to a synchrotron peak which has been observed in the X-ray range. This allows us to determine jet parameters which may explain the variability and spectrum of Mkn 501. We discuss the implications of this spectrum in the context of the synchrotoron self-Compton source hypothesis (Stecker, de Jager & Salamon 1996) and for constraints on the breaking of Lorentz invariance.

# 2. A Hybrid SED for the IR-optical Intergalactic Radiation Field

In order to recalculate the  $\gamma$ -ray opacity of intergalactic space from photon-photon pair production interactions, we adopt a hybrid model which uses the near-IR to far-IR background SED calculated by Malkan & Stecker (2001) combined with a reasonable, smooth extention into the optical-UV wavelength range derived from recent HDF (Hubble Deep Field) galaxy counts by Madau & Pozzetti (2001). We will refer to the entire FIR-UV background as the EBL (extragalactic background light).

Malkan & Stecker (2001) have used their empirically based model (Malkan & Stecker 1998) to predict infrared galaxy luminosity functions and deep infrared galaxy counts at various wavelengths. They have also examined their predictions for the IR SED for comparison with the subsequent determinations from the *COBE-DIRBE* data analysis. Using the assumption of pure luminosity evolution proportional to  $(1 + z)^Q$  out to a redshift of  $z_{flat}$  and constant (no evolution) for  $z_{flat} < z < z_{max} = 4$ , they find that a comparison of their predictions with current *ISO* galaxy counts at 15 and 175  $\mu$ m favor their "baseline model" with Q = 3.1 and  $z_{flat} = 2$  (the lower curve in Figure 1). The mid-IR  $\gamma$ -ray upper limits of  $\sim 4-5$  nW m<sup>-2</sup>sr<sup>-1</sup> (Stecker & De Jager 1997; Stanev & Franceschini 1998; Renault, *et al.* 2001) also favor  $Q \sim 3$ .

On the other hand, the *COBE-DIRBE* far infrared background flux determinations of Hauser *et al.* (1998) seem to favor a stronger evolution with Q > 4 up to  $z_{flat} = 1.^1$  The upper curve in Figure 1, which shows the "fast evolution" model of Malkan & Stecker (2001), assumes Q = 4.1 and  $z_{flat} = 1.3$ . The lower curve in Figure 1 shows the baseline model.

If one rederives the 140  $\mu$ m and 240  $\mu$ m background fluxes from *COBE-DIRBE* using the *COBE-FIRAS* calibration, which suffered from smaller systematic errors than the *COBE-DIRBE* calibration (Fixsen *et al.* 1997), the fluxes are lowered to the point where they are *consistent with both* the baseline and fast evolution SEDs of Malkan & Stecker (2001) (see Figure 1). The newly derived flux at 170  $\mu$ m obtained from *ISOPHOT* maps by Kiss *et al.* (2001), also shown in Figure 1, is also consistent with the both Malkan-Stecker SEDs. In this regard, one should also note that the results reported by Hauser *et al.* (1998) were at the  $4\sigma$  level. (See Malkan & Stecker (2001) for further discussion.)

Our hybrid approach extends the IR SEDs of Malkan & Stecker (2001) to shorter wavelengths by exploiting the fact that the Hubble Deep Field (HDF) was able to resolve the lowest intensity galaxies. In other words, a graph of the integral number of galaxies above a given intensity as a function of that intensity shows convergence to a constant value, which

<sup>&</sup>lt;sup>1</sup>There was a tentative derivation of the background at 60  $\mu$ m and 100  $\mu$ m by Finkbeiner, Davis & Schlegel (2001). However, this result now appears to have suffered from contamination by local solar system dust emission (Finkbeiner 2001).

implies that the total amount of extragalactic background light (EBL) has been captured in the wavebands of interest. Thus, unless there are significant non-stellar, intergalactic contributions to the optical background or very low surface brightness galaxies missed by the *HST* (Hubble Space Telescope), the flux derived from the HDF should represent the true EBL.

Galaxy counts provide a strict lower limit on the intensity of the EBL, since faint or unresolved galaxies not included in the counts are additional contributors to the EBL. The relative importance of the unresolved sources compared to that of the resolved sources can be estimated from fluctuation analyses of the EBL. A lack of fluctuations will suggest a certain degree of completeness in the source counts. Based on such fluctuation analyses, the intensities reported by Madau & Pozzetti (2001) can be considered as actual detections of the EBL at the wavelengths studied. Their results are shown as such in Figure 1. These authors also give a lower limit of 15 nW m<sup>-2</sup>sr<sup>-1</sup> for the integrated light between 0.2 and  $2.2 \ \mu$ m.<sup>2</sup>

The HDF K–band (2.2  $\mu$ m) flux is further complemented by ground based observations. Gardner (1996) gives a lower limit of 7.4 nW m<sup>-2</sup> sr<sup>-1</sup> on the EBL intensity, but deeper K-counts (Bershady, Lowenthal & Koo 1998) suggest an increase in the K > 23 counts over previous surveys (see *e.g.* Gardner 1996). The slope in the K-band counts, dN/dm is about 0.36. Adopting a slope of 0.4 down to K = 30 magnitudes, E. Dwek (1999, personal communication) derived a conservative upper limit of 13 nW m<sup>-2</sup> sr<sup>-1</sup> for the EBL intensity in the K-band. These two limits are shown as a thick vertical bar in Figure 1 and provide an important constraint when attempting to connect the far-IR to UV parts of the EBL in any hybrid model. From Figure 1 we also see that the ground based limit on the K-band flux is consistent with the *HST* galaxy counts in the HDF. Dwek and Arendt (1998) have used *COBE-DIRBE* data to derive a tentative estimate of the EBL flux at a wavelength of 3.5  $\mu$ m of 9.9 ± 5.8 (2 $\sigma$ ) nW m<sup>-2</sup>sr<sup>-1</sup>, shown by the solid diamond point in Figure 1, which is also seen to be in good agreement with our models.

It can be seen from Figure 1 that the Malkan & Stecker (2001) models connect smoothly with the near-IR to UV lower limits for the EBL based on HDF galaxy counts (Madau & Pozzetti 2001). This fact allows us to construct a reasonable *hybrid model*, smoothly extending the infrared model SEDs of Malkan & Stecker (2001) to UV wavelengths.

The thick curves in Figure 1 show the SEDs predicted by the baseline (lower curve)

<sup>&</sup>lt;sup>2</sup>There is evidence for an upturn in the SED at the shortest observed UV wavelengts near  $2 \times 10^{15}$  Hz as derived from the *HST* imaging spectrograph (Gardner, Brown and Ferguson 2000), but this feature does not significantly affect our absorption calculations; the UV background only affects ~ 50 to 100 GeV  $\gamma$ -rays from sources at high redshifts (Salamon & Stecker 1998).

and fast evolution models (upper curve) of Malkan & Stecker (2001). The baseline SED of Malkan & Stecker (2001) connects smoothly with the mean stellar component (open circles) derived from galaxy counts (*HST* and ground–based), which is shown as the thin dashed line (lower curve in Figure 1). The integral of this spectrum (extending through the mean UV to K–band fluxes) between 0.2  $\mu$ m and 2.2  $\mu$ m gives a value of 16 nW m<sup>-2</sup>sr<sup>-1</sup>, which is just above the galaxy count lower limit of 15 nW m<sup>-2</sup>sr<sup>-1</sup> derived by Madau & Pozzetti (2001). The fast evolution model of Malkan & Stecker (2001) also runs smoothly through the  $2\sigma$  galaxy count limits and gives us a reasonable upper limit for the EBL in the UV to far-IR.

Figure 1 summarizes the observationally derived values for the optical-UV, near-IR and far-IR fluxes which now exist. Unfortunately, foreground emission prevents the direct detection of the EBL in the mid-IR wavelength range (See discussion in Hauser & Dwek 2001.) However, we note that other theoretical models such as those of Tan, Silk & Balland (1999), Rowan-Robinson (2000) and Xu (2000) predict fairly flat SEDs in the mid-infrared range with average flux levels in the 3 to 4 nW m<sup>-2</sup>sr <sup>-1</sup> as do the Malkan & Stecker (2001) models used here. These flux levels are also consistent with the indirect mid-IR constraints indicated by the box in Figure 1 (These constraints are summarized by Stecker (2001). Fine detailed differences between these theoretical SEDs are not important in determining the optical depth of intergalactic space to high energy  $\gamma$ -rays,  $\tau(E, z)$ , (see next section) because its determination involves integrating over a significant range of EBL wavelengths (Stecker, et al. 1992). As an example of this, we note that Vassiliev (2000) has shown that for a flat SED, 90% of the contribution to the  $\gamma$ -ray optical depth is contributed by EBL photons of wavelengths between .28 and 2.7 times the optimum wavelength corresponding to the peak in the pair production cross section. This is roughly an order of magnitude in integrated EBL wavelengths.

We therefore assert that the two Malkan & Stecker curves, extended into the optical-UV range by our hybrid model, give a reasonable representation of the EBL in the UV to far-IR. Other EBL models in the literature whose flux levels roughly fit the present data and have the same spectral characteristics, *i.e.*, a stellar optical peak, a far-IR dust emission peak, and a mid-IR valley which allows for some warm dust emission (see review of Hauser & Dwek 2001), should give similar results on the optical depth of the near Universe  $\tau(E, z)$  to high energy  $\gamma$ -rays (see next section).

# 3. The Optical Depth for Very High Energy $\gamma$ -rays from sources at z < 0.3.

We used the prescription of Stecker & de Jager (1998), together with the hybrid model discussed in the previous section, to recalculate the optical depth of intergalactic space  $\tau(E, z)$  for redshifts between 0.03 (near the z values of Mkn 501 and 421) and 0.3, assuming that the EBL is in place by a time corresponding to z = 0.3. Above  $z \sim 0.3$ , evolutionary effects have to be taken into account (Salamon & Stecker 1998). Figure 2 shows  $\tau(E, z)$ calculated using the baseline and fast evolution models for  $\gamma$ -ray energies down to  $\sim 50$  GeV, which is the approximate threshold energy for meaningful image analyses in next generation ground based  $\gamma$ -ray telescopes such as *MAGIC*, *H.E.S.S.* and *VERITAS*. Where our results overlap, they are in good agreement with the metallicity corrected results of Salamon & Stecker (1998). We note that the Salamon & Stecker (1998) results extend to both lower energies and higher redshifts.

As a quantitative example of the uncertainty in the predicted value of  $\tau(E)$  at the Mkn 501 redshift of 0.031 produced by the uncertainty in the EBL flux, we note that the 19% difference between our two model curves at the mid-IR wavelength of 10  $\mu$ m (see Figure 1) maps into a difference of 21% in the optical depth at 10 TeV (see Figure 2). This, in turn yields a difference of 34% in the predicted Mkn 501 intrinsic  $\gamma$ -ray flux at 10 TeV. The uncertainty in the energy above which the optical depth is greater than 1 is indicated in Figure 2. We find that  $\tau(E) \geq 1$  for  $E \geq 2.3$  TeV assuming the "fast evolution" model for the EBL and  $\tau(E) \geq 1$  for  $E \geq 3.2$  TeV for the baseline model EBL.

As in Stecker & de Jager (1998), we also obtained parametric expressions for  $\tau(E, z)$  (as shown in Figure 2), but the accuracy was improved by increasing the order of the polynomials. The expressions are of the form (for z < 0.3 and  $0.1 < E_{\text{TeV}} < 50$ ):

$$log_{10}[\tau(E_{\text{TeV}}, z)] \simeq \sum_{i=0}^{4} a_i(z) (\log_{10} E_{\text{TeV}} + 2)^i$$
 (1)

where the z-dependent coefficients are given by

$$a_i(z) = \sum_{j=0}^3 a_{ij} (\log_{10} z)^j.$$
<sup>(2)</sup>

Tables 1 (baseline model) and 2 (fast evolution, numbers in brackets) give the numerical values for  $a_{ij}$ , with j = 0, 1, 2, 3, and i = 0, 1, 2, 3, 4. Equation (2) approximates  $\tau(E, z)$  correctly within 5% for all bounded values of z and E considered.

#### 4. The Observed Spectrum of Mkn 501 during the 1997 Flare.

Recently the *HEGRA* group (Aharonian *et al.* 2001a) rederived the energy spectrum of Mkn 501 during the 1997 flare. The validity of the high energy tail of the spectrum out to 20 TeV in their earlier analysis (Aharonian *et al.* 1999) was questioned because of spillover effects between energy channels. A reanalysis of the events above 3 TeV with better energy resolution gave a flux at  $\sim 21$  TeV which was a factor of 3.6 lower than that obtained in their previous analysis. It should be stressed that their revised spectrum is consistent with the original spectrum below 20 TeV. The final spectrum between 0.56 and 21 TeV is shown in Figure 3 and marked "OBSERVED".

Contemporaneous observations of Mkn 501 by the *Whipple* group (Krennrich *et al.* 1999) are consistent (within errors) with the *HEGRA* spectrum in the overlapping energy range between 0.5 and 10 TeV. This allows us to add the two *Whipple* points below 0.5 TeV to the *HEGRA* spectrum, giving an observed spectrum between 0.26 and 22 TeV for the Mkn 501 flare. The result is a single spectrum extending over two decades of energy as shown in Figure 3.

#### 5. The Intrinsic VHE Spectrum of Mkn 501 during the 1997 Flare.

By using both the Whipple and *HEGRA* spectra of Mkn 501 and correcting for absorption by multiplying by  $e^{\tau(E)}$  evaluated at z = 0.034 with the newly derived values for the opacity calculated as discussed in the previous section, we have derived the intrinsic spectrum of Mkn 501 over two decades of energy. This is given by the data points and two curves marked INTRINSIC in Figure 3. The upper of these curves corresponds to the fast evolution case; the lower curve corresponds to the baseline model case.

Fossati *et al.* (2000) suggested a parameterization to describe smoothly curving blazar spectra. This parameterization is of the form

$$\frac{dN}{dE} = KE^{-\Gamma_1} \left( 1 + \left(\frac{E}{E_B}\right)^f \right)^{(\Gamma_1 - \Gamma_2)/f} \tag{3}$$

A spectrum of this form changes gradually from a spectral index of  $\Gamma_1$  to an index of  $\Gamma_2$ when the energy E increases through the break energy  $E_B$ . The parameter f describes the rapidity ("fastness") of the change in spectral index over energy. This model was used by Fossati *et al.* (2000) to describe the curvature in the Mkn 421 spectrum. We have fitted our derived intrinsic Mkn 501 spectrum to the form given by equation (3).

We applied the formalism of Fossati *et al.* (2000) and found the best-fit parameters K,  $E_B$ , f,  $\Gamma_1$  and  $\Gamma_2$  after correcting the observed spectrum for intergalactic absorption. A total

of 27 data points between 0.26 ad 21 TeV were used for each of the two intrinsic spectra in Figure 3, and we fitted to the Fossati *et al.* parameterization of these spectra, keeping all parameters free. Whereas the low energy spectral index  $\Gamma_1$  appears to be well constrained, we find that the higher energy index  $\Gamma_2$  is unconstrained. Table 3 shows the parameter values for each fit, assuming two arbitrary values for  $\Gamma_2$  (2.5 and 3.0). The parameter  $E_M$  is derived from the fit, and corresponds to the  $\gamma$ -ray energy where the SED peaks in  $\nu F_{\nu}$ . The fits are acceptable in terms of the  $\chi^2$  per degree of freedom.

It is important to note that the intrinsic spectrum which we derive does not have an upturn near 20 TeV as obtained previously by some authors (e,g. Protheroe & Meyer 2000; Dwek 2001) working with the earlier analysis of Aharonian, et al. (1999) as well as the 60  $\mu$ m flux earlier reported by Finkbeiner et al. (2000 - see footnote 1). The upturn obtained by Dwek (2001) can be effectively eliminated by using the revised HEGRA  $\gamma$ -ray data with the observed flux reduced by a factor of 4 at ~20 TeV; the stronger upturn obtained by Protheroe & Meyer (2001) is eliminated both by using the revised HEGRA data and a more realistic IR-SED than the one these authors used which had no mid-IR valley and an unreasonably high mid-IR flux.

Aharonian, Timokhin & Plyasheshnikov (2001b) have also found an upturn in their analysis, particularly if they use an SED constructed using the flux claimed by Lagache *et al.* (2000) at 100  $\mu$ m, the only point in Figure 1 which is inconsistent with our SEDs at the  $2\sigma$  level. Assuming that this upturn is correct, these authors suggested avoiding a "TeV-IR crisis" by invoking a cold jet near the central engine with a bulk Lorentz factor greater than  $10^7$ , with the upturn resulting from comptonization.

In this context, we note that the *COBE-DIRBE* group has argued that a real flux derived from the *COBE-DIRBE* data at 100  $\mu$ m, as claimed by Lagache *et al.* (2000), is untenable because isotropy in the residuals (after foreground subtractions) could not be proven. Dwek *et al.* (1998) have concluded that only a conservative lower limit of 5 m<sup>-2</sup>sr<sup>-1</sup> could be inferred at 100  $\mu$ m. For Model II of Aharonian *et al.* (2001b) which neglects the 100  $\mu$ m point, these authors derive a source spectrum which is *quite flat up to an energy of* ~ 20 *TeV*, as we do in this work. This obviates any need to invoke extreme bulk Lorentz factors in modelling the Mkn 501 source spectrum.

Our intrinsic SED is slightly convex, rather than a single power law, consistent with an SSC hypotheses for the origin of the TeV radiation. We find that this SED peaks at  $E_M \sim 8-9$  TeV (independent of the unconstrained  $\Gamma_2$ ) in the case where the fast evolution EBL is assumed and that  $E_M \sim 5$  TeV if the baseline EBL is assumed (see Figure 3 and Table 3.)

# 6. A Simple Interpretation of the Intrinsic Mkn 501 Flare Spectrum within the Context of the SSC Paradigm

If one observationally determines a flaring variability time  $\Delta t$ , the optical depth for  $\gamma - \gamma$  absorption from pair production is then given by (Dermer & Schlickheiser 1994; Aharonian, *et al.* 1999)

$$\tau_{\gamma\gamma} \simeq 0.055 \phi_{10} \Delta t_{\rm day}^{-1} \delta_{10}^{-6} H_{65}^{-2} E_{\rm TeV} \tag{4}$$

using the normalizations  $\delta_{10} \equiv \delta/10$  and  $\phi_{10} \equiv \phi_r/10^{-10}$  erg cm<sup>-2</sup>s<sup>-1</sup> with  $\phi(\epsilon) \equiv \epsilon^2 (dN/d\epsilon)$ being the observed energy flux of the low energy radiation. The flux  $\phi(\epsilon)$  is determined at  $\epsilon \sim 100\delta_{10}^2 E_{\text{TeV}}^{-1}$  eV which is the energy range of the low energy photons responsible for the intrinsic optical depth of high energy  $\gamma$ -rays in the jet. The value of the relevant low energy radiation flux  $\phi_{10}$  is approximately 0.5 in the optical–UV range.  $H_{65}$  is the Hubble constant is in units of 65 km s<sup>-1</sup> Mpc<sup>-1</sup>.

The time variation of the TeV  $\gamma$ -ray flux scales as the square of the time variation of the X-ray flux. This scaling favours a synchrotron-self Compton origin for the Mkn 501 source with the synchrotron peak in the X-ray range and the Compton peak in the TeV  $\gamma$ -ray range (Krawczynski, *et al.* 2000). The X-ray SED of Mkn 501 appears to have a maximum in the  $\sim$  50-100 keV range in the synchrotron component (Catanese *et al.* 1997; Pian *et al.* 1998; Petry, *et al.* 2000). This shape should be reflected in the high energy  $\gamma$ -ray domain, but with different fastness (f) and slopes ( $\Gamma_1$  and  $\Gamma_2$ ) owing to the energy dependence of the cross section for inverse Compton scattering as the possibility of having more than one soft target photon component for such scattering (Stecker, De Jager & Salamon 1996).

Since Mkn 501 is a giant elliptical galaxy with little dust, it is also reasonable to assume that the galaxy itself does not produce enough infrared radiation to provide a significant opacity to high energy  $\gamma$ -rays. Also, if our EBL is approximately correct, it is reasonable to assume that the dominant absorption process is intergalactic and that pair-production in the jet in negligible. This hypothesis is supported by the fact that the high energy  $\gamma$ -ray SED did not steepen during the flare. This implies that the optical depth given by eq. (4) is less than unity out to the highest observed energy  $E \sim 20$  TeV. The pair-production opacity constraints then limit the Doppler factor to

$$\delta_{10} \simeq 1.2 \left(\frac{\phi_{-10}}{0.5}\right)^{1/6} \left(\frac{5 \text{ hours}}{\Delta t}\right)^{1/6} H_{65}^{-1/3} \left(\frac{E_{\gamma}}{20 \text{ TeV}}\right)^{1/6}$$
(5)

which is consistent with the lower limit of  $\delta_{10} = 1$  set by Aharonian *et al.* (1999).

The energy of the synchrotron peak in the X-ray region is given by

$$E_{X,M}(\text{keV}) \simeq 67B_{0.1}\delta_{10}[E_e(\text{TeV})]^2$$
 (6)

where  $E_e$  is the energy of the electrons which are radiating into the synchrotron peak and  $B_{0.1}$  is in units of 0.1 G. The energy of the Compton peak in the Klein-Nishina range is given by

$$E_M = \delta \kappa E_e \tag{7}$$

where the inelasticity factor,  $\kappa \sim 1$  in the Klein-Nishina limit.

From equations (4) and (5), we obtain the SSC expression for  $E_M$ ,

$$E_M(\text{TeV}) \simeq 1.2\kappa \delta_{10}^{1/2} B_{0.1}^{-1/2} E_{X,M} (\text{keV})^{1/2}.$$
 (8)

Note that this expression also holds if SEC is important. Krawczynski *et al.* (2000) have estimated the *B* field from the observed lag in the cooling time between the 3 keV and 12 keV synchrotron radiation in the jet to be  $\geq 0.025$  G.

Taking  $\delta_{10} \sim 1$ ,  $B_{0.1} = 1$ ,  $\kappa \sim 1$  and 50 keV  $\leq E_{X,M} \leq 100$  keV (Pian, *et al.* 1998) then eq. (8) gives a prediction of  $E_{TeV,M} \sim 9 - 12$  TeV, in good agreement with the results of the  $\chi^2$  fit to our intrinsic SED for the Mkn 501 flare of  $\sim 5 - 9$  TeV. (Note that this value only depends on the square roots of the parameters involved.)

It should be noted that Tavecchio, *et al.* (1998) neglected intergalactic absorption and used the observed spectrum of Mkn 501 with an assumed Compton peak at sub-TeV energies to determine constraints on SSC jet parameters. The fact that they failed to derive a self-consistent model shows the importance of taking intergalactic absorption into account in theoretical work involving TeV blazars.

Our interpretation is based on *time averages* of flare spectra measured during the 1997 high state. However, our analysis is validated by the analyses of Petry *et al.* (2000). These authors also compared the TeV data with the soft- and hard X-ray data after averaging the X-ray data over several flares during the same high state. Our comparison uses both the soft X-ray spectral index and the hard X-ray peak taken from the Petry *et al.* (2000) averages.

# 7. Conclusions

The IR SEDs which Malkan & Stecker (2001) have derived and argued are consistent with all of the reliable data on the IR EBL connect smoothly with the EBL derived from converging galaxy counts in the near-IR to UV. Furthermore, at the longest wavelengths, they also connect smoothly with the *COBE-FIRAS* results. This allows us to construct hybrid EBL SEDs which were used to recalculate the optical depth versus redshift for high energy  $\gamma$ -rays between 50 GeV and 100 TeV, the energy above which the Universe becomes highly opaque, even at low redshifts, owing to interactions with photons of the 2.7K cosmic background radiation (Stecker 1969).

We find that our derived intrinsic flaring SED for Mkn 501 exhibits a broad maximum in the  $\sim 5-10$  TeV range, which is consistent with a value of  $\sim 10$  TeV predicted from several consistent physical arguments and independent observational constraints for the SSC model (see previous section). The Mkn 501 SED derived in this paper does not show the upturn above  $\sim 20$  TeV found in some other studies. We agrue here that such a feature is an artifact produced partly by spillover in the last data bin in the original *HEGRA* analysis and partly by assuming too high an IR background SED.

Our differential photon spectral index,  $\Gamma_1$ , for the energy range  $E_{\gamma} \ll E_{\rm M}$  is 1.6 to 1.7 (Table 3), which is close to the differential photon spectral index of 1.76 at soft X-ray energies (Petry *et al.* 2000). The similarity of these spectral indices implies that  $\gamma$ -rays below ~ 1 TeV are produced in the Thomson regime by scattering off soft photons with energies in the optical-IR range. On the other hand,  $\gamma$ -rays near the ~ 7 ± 2 TeV Compton peak are the result of scattering in the Klein-Nishina range (see previous section).

Our derived intrinsic Mkn 501 SED is quite flat in the multi-TeV range as shown in Figure 3. This is in marked contrast to the dramatic turnover in its observed SED. We argue that this is strong evidence that the observed spectrum shows just the absorption effect predicted. Among other consequences of this conclusion, the observed absorption feature allows one to put strong constraints on the breaking of Lorentz invariance (Stecker & Glashow 2001).

Acknowledgment: We would like to thank Felix Aharonian, Eli Dwek and Karl Mannheim for useful discussions.

# REFERENCES

Aharonian, F.A. et al., 1999, A&A, 349, 11

Aharonian, F.A. et al., 2001a, A&A, 366, 62

Aharonian, F.A., Timokhin, A.N. & Plyasheshnikov, A.V., 2001b, submitted to A&A, e-print astro-ph/0108419

Bershady, M.A., Lowenthal, J.D. & Koo, D.C., 1998, ApJ, 505, 50

- Catanese, M., Bradbury, S.M., Breslin, A.C., et al., 1997, ApJ, 487, L143
- Dermer, C.D., & Schlickeiser, R., 1994, ApJ Suppl., 90, 945
- Dwek, E. 2001, in *The Extragalactic Infrared Background and its Cosmological Implications*, *IAU Symposium no. 204* ed. M. Harwit and M.G. Hauser, p. 389
- Dwek, E & Arendt, R.G. 1998, ApJ 508, L9
- Dwek, E. et al. 1998, ApJ 508, 106
- Elbaz, D., Cesarsky, C.J., Fadda, D., et al., 1999, A&A, 351, L37
- Finkbeiner, D.P. 2001, in The Extragalactic Infrared Background and its Cosmological Implications, IAU Symposium no. 204 ed. M. Harwit and M.G. Hauser, p. 121
- Finkbeiner, D.P., Davis, M., & Schlegel, D.J. 2000, ApJ, 544, 81
- Fixsen, et al. 1997, ApJ 490, 482
- Fixsen, D.J., Dwek, E., Mather, J.C. 1998, Bennett, C.L. & Shafer, R.A., ApJ, 508, 123
- Fossati, G., Celotti, A., Chiaberge, M., et al., 2000, ApJ, 541, 166
- Gardner, J.P. in Unveiling the Cosmic Infrared Background, ed. E. Dwek (New York: AIP Press) (1996) p.127
- Gardner, J.P., Brown, T.M., & Ferguson, H.C., 2000, ApJ, 542, L79
- Gispert, R., Lagache, G., & Puget, J.L., 2000, A&A, 360, 1
- Guy, J., Renault, C., Aharonian, F. A., Rivoal, M. & Tavernet, J.-P. 2000, A&A, 359, 419
- Hauser, M.G., et al., 1998, ApJ, 508, 25
- Hauser, M.G. & Dwek, E., 2001, ARA&A, 39, 249
- Konopelko, A.K., Kirk, J.G., Stecker, F.W. & Mastichiadis, A., 1999 ApJ, 518, L13
- Kiss, Cs., Abraham, P., Klass, U., Juvela, M. & Lemke, D. 2001, A & A, in press, e-print astro-ph/0110143
- Krawczynski, H., Coppi, P.S., Maccarone, T. & Aharonian, F.A. 2000, A&A 353, 97
- Krennrich, F. et al., 1999, ApJ, 511, 149

- Lagache, G., Hafner, L.M., Reynolds, R.J. & Tufte, S.L. 2000, A&A 354, 247.
- Madau, P., & Pozzetti, L., 2001, MNRAS, 312, L9
- Malkan, M.A. & Stecker, F.W. 1998, ApJ 496, 13
- Malkan, M.A. & Stecker, F.W. 2001, ApJ 555, 641
- Petry, D. et al. 2000, ApJ, 536, 742
- Pian, E. et al. 1998, ApJ 492, L17
- Protheroe, R.J. & Meyer, H. 2000, Phys. Letters 493, 1
- Renault, C., Barrau, A., Lagache, G., & Puget, J.-L., 2001, A&A, 371, 771
- Rowan-Robinson, M. ApJ 549, 745
- Salamon, M.H. & Stecker, F.W. 1998, ApJ 493, 547
- Stanev, T., & Franceschini, A., ApJ, 494, L159
- Stecker, F.W. 1969, ApJ 157, 507
- Stecker, F.W. 2001, in The Extragalactic Infrared Background and its Cosmological Implications, IAU Symposium no. 204 ed. M. Harwit and M.G. Hauser, p. 135
- Stecker, F.W. & de Jager, O.C. 1997, in Towards a Major Atmospheric Cerenkov Detector V, Proc. Kruger Natl. Park Workshop on TeV Gamma-Ray Astrophysics ed. O.C. de Jager (Potchefstoom: Wesprint), p. 39, e-print astro-ph/9710145
- Stecker, F.W. & de Jager, O.C. 1998 A&A, 334, L85
- Stecker, F.W. de Jager, O.C. & Salamon, M.H. 1992, ApJ, 390, L49
- Stecker, F.W. De Jager, O.C. & Salamon, M.H. 1996, ApJ, 473, L75
- Stecker, F.W. & Glashow, S.L. 2001, Astroparticle Phys. 16, 97
- Tan, J.C., Silk, J. & Balland, C. 1999, ApJ 522, 579
- Tevecchio, F. et al. 1998, ApJ 509, 608
- Vassiliev, V.V. 2000, Astropart. Phys. 12, 217
- Wright, E.L., & Reese, E.D., 2000, ApJ, 545, 43

Xu, C. 2000, ApJ 541, 134

This preprint was prepared with the AAS  ${\rm IAT}_{\rm E}{\rm X}$  macros v3.0.

# **Figure Captions**

Figure 1. The SED of the EBL (see text for references and descriptions). All error bars given at the  $\pm 2\sigma$  level. The Malkan & Stecker (2001) fast evolution model is shown by the upper, thick solid curve between  $\log_{10} \nu = 11.8$  to 13.8) and their baseline model is shown by the thick dashed line over the same frequency range. Convergent Hubble Deep Field galaxy counts (Madau & Pozzetti 2001): open circles; Ground–based galaxy counts limits at 2.2 $\mu$ m (see text): thick vertical bar marked "2.2 $\mu$ "; COBE-DIRBE photometric sky residuals (Wright & Reese 2000): small open squares; TeV  $\gamma$ -ray-based upper limits: thick box marked "TeV" (see text for references); ISOCAM lower limit at 15 $\mu$ m: upward arrow marked 15 $\mu$  (Elbaz et al. 1999); COBE-DIRBE far-IR sky residuals (Hauser et al. 1998): large open squares at 140  $\mu$ m and 240  $\mu$ m; COBE-DIRBE data recalibrated using the COBE- FIRAS calibration (see text): large solid squares without error bars; ISOCAM 170  $\mu$ m flux (Kiss et al. 2001): solid circle; COBE-FIRAS far-IR sky residuals (Fixsen, et al. 1998): thick dot-dash curve with ~ 95% confidence band (thin dot–dash band); 100 $\mu$ m COBE-DIRBE point (Lagache et al. 2000): small solid square; flux at 3.5  $\mu$ m from COBE-DIRBE (Dwek & Arendt 1998): solid diamond.

Figure 2. The optical depth for  $\gamma$ -rays above 50 GeV given for redshifts between 0.03 and 0.3 (as labelled) calculated using the medium (dashed lines) and fast evolution (solid lines) SED of Malkan & Stecker (2001).

Figure 3. The observed spectrum and derived intrinsic spectrum of Mkn 501. The observed spectral data are as measured by *HEGRA* (solid circles) and *Whipple* (solid squares). The upper points are the absorption corrected data points (marked "INTRINSIC") using our fast

i	$a_{i0}$	$a_{i1}$	$a_{i2}$	$a_{i3}$			
0	-5.1512	-4.4646	-3.5143	-0.80109			
1	9.2964	16.275	10.7540	2.51610			
2	-4.8645	-12.86	-8.6982	-2.07510			
3	1.1164	3.9795	2.747	0.66596			
4	-0.084039	-0.42147	-0.29644	-0.072889			

Table 1: Polynomial coefficients  $a_{ij}$  for the baseline model.

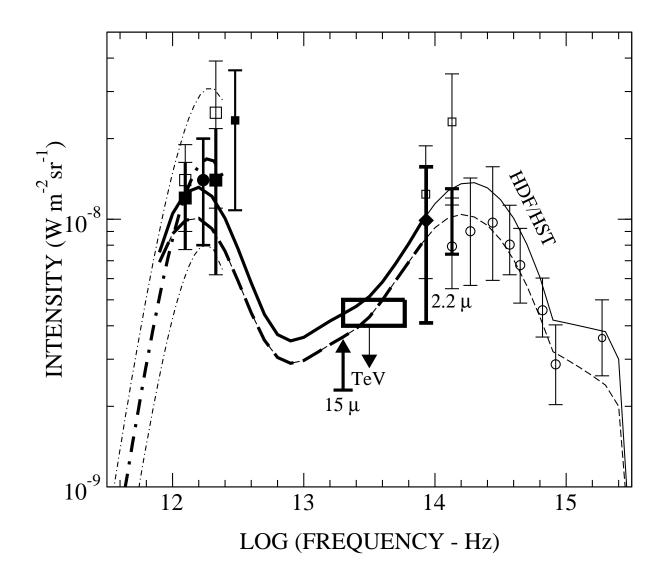
i	$a_{i0}$	$a_{i1}$	$a_{i2}$	$a_{i3}$
0	(-5.4748)	(-4.7036)	(-3.5842)	(-0.79882)
1	(10.444)	(17.114)	(11.173)	(2.58430)
2	(-5.8013)	(-13.733)	(-9.2033)	(-2.17670)
3	(1.4145)	(4.3143)	(2.9535)	(0.71046)
4	(-0.11656)	(-0.46363)	(-0.32339)	(-0.078903)

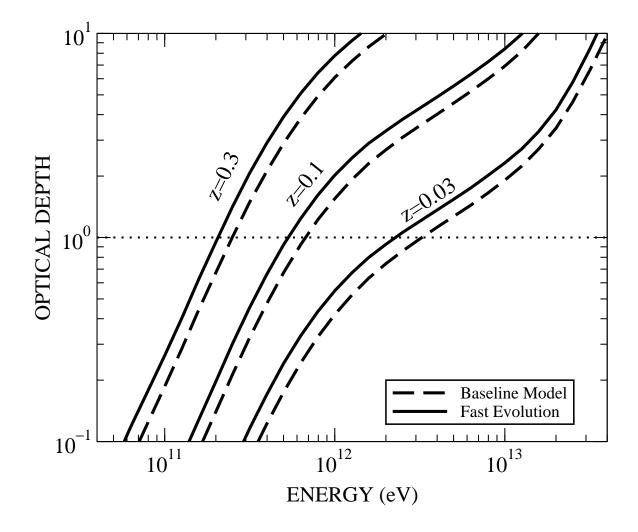
Table 2: Polynomial coefficients  $a_{ij}$  for the fast evolution model.

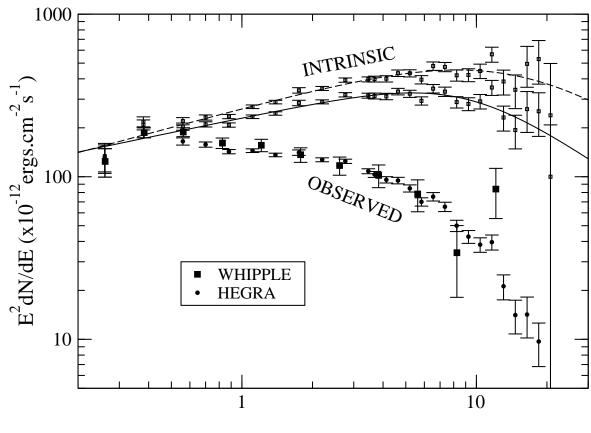
Table 3: Results of a multiparameter fit of a continuous curvature model to the absorption corrected differential photon fluxes dN/dE of Mkn 501 during its 1997 high state. Errors are typically on the last digit.

T	V	0						
	EBL	$K \; (\times 10^{-10})$	f	$E_B$	$\Gamma_1$	$\Gamma_2$	$\chi^2/dof$	$E_M$
	Model	$(\mathrm{ergs}\ \mathrm{cm}^{-2}\mathrm{s}^{-1})$		$(\mathrm{TeV})$				$(\mathrm{TeV})$
	Fast Evolution	2.64	1.6	15.0	1.61	3.0	1.26	9.0
	Fast Evolution	2.62	2.1	8.8	1.62	2.5	1.24	7.9
	Baseline	2.30	2.3	9.0	1.70	3.0	1.32	4.7

evolution hybrid EBL (upper data set and solid curve fit) and baseline hybrid EBL (lower data set with dashed curve fit). The fit parameters are given in Table 1.







ENERGY (TeV)